Controlled Suppression or Amplification of Turbulent Jet Noise

D. F. Long,* H. Kim,† and R.E.A. Arndt‡
University of Minnesota, Minneapolis, Minnesota

As a result of acoustic excitation under very specific tuned conditions, both amplification and suppression of the broadband component of jet noise can be achieved in the same test rig. Associated with the amplification are discrete tones corresponding to the subharmonics of the excitation at the shear layer instability frequency. When jet noise is suppressed, flow visualization indicates that the turbulent mixing is less intense resulting in a general elongation of the jet flow in the axial direction. The observation of reduced jet spreading is confirmed by sound source distribution measurements using a polar correlation technique. Under these conditions, the axial source distribution is shifted downstream by approximately two diameters.

Nomenclature

D = jet diameter
f_a = interaction tone
f_c = column mode frequency
f_e = excitation frequency
f_s = shear layer instability frequency
M = Mach number
Re = Reynolds number
St = Strouhal number
U = jet velocity
α = directivity angle
β = separation angle in a meridian plane (fixed microphone location at $\alpha = 90$ deg)
θ = exit momentum thickness

Introduction

THIS paper describes measurements of the sound radiating from an acoustically excited, low Mach number jet. The experiment is carried out under very special conditions. The jet is "tuned" by adjusting the velocity such that the frequency of the most unstable mode in the shear layer is eight times the dominant fluctuation frequency observed near the end of the potential core. This tuned condition is illustrated schematically in Fig. 1. The shear-layer frequencies of interest are bracketed by the Strouhal number range, based on momentum thickness of the shear layer, of $0.013 < St_\theta < 0.017$. Since the boundary layer at the nozzle is laminar, the instability frequencies vary with the three-halves power of velocity, $U^{3/2}$. On the other hand, the most unstable frequency in the potential core, f_c, has a constant Strouhal number based on nozzle diameter of $St_D \sim 0.5$ and, hence, this frequency varies with the first power of velocity. The intersection of the line representing $8f_c$ with the lines denoting the unstable shear layer frequencies delineates the region of interest.

The flow conditions were varied around this tuned condition. In one case the exit velocity was maintained constant and the excitation frequency was varied. In the other case the excitation frequency was maintained constant and the exit velocity was varied. The range of these cases is shown by the horizontal and vertical dotted lines on Fig. 1. It is extremely important to note that the jet is only sensitive to the excitation in this region. Outside of this region the excitation has no effect on the jet. Within this region a variety of phenomena are observed and will be described later.

The coupling between relatively high-frequency shear-layer instabilities and a relatively low-frequency column-mode instability has been previously observed by Kibens[1] in the radiated noise. He postulated that coupling occurred through the vortex pairing process. Each pairing halves the instability frequency. If, after several pairings, the shear-layer frequency matches the column mode instability frequency, then coupling occurs. In other words, the jet is tuned when $f_s = 2^n f_c$, n is an integer. Under the present experimental conditions, coupling occurs when $n = 3$.

Experimental Conditions

The experimental conditions are as follows: $D = 7.1$ mm, $U = 56$-92 m/s, $\theta = \sim 2.8 \times 10^{-2}$ mm, $f_e = 39 \sim 51$ kHz, $f_c = \sim 5$ kHz, $Re = \sim 35 \times 10^3$, $M = \sim 0.21$, $St_\theta = 0.013 \sim 0.017$. The exit-momentum thickness was too small to be measured with hot-wire anemometry. It was determined from the Karman momentum integral equation using the potential flow solution through the nozzle as the outer flow velocity.

The facility is the same as that used by Long and Arndt.[2] A 7.1-mm nozzle exhausts into an anechoic chamber that measures 2.2 m on a side. In order to excite the initial shear layer at the high frequencies involved, an excitation chamber is fitted around the nozzle (see Fig. 2). The chamber is driven by a 6-mm B & K microphone used as a sound source mounted in the side. A thin slit at the nozzle exit allows the pressure fluctuations within the chamber to impinge on the initial shear layer around the entire jet.

The chamber was constructed with the hope that it would respond to the excitation under pressure conditions (Frederiksen[3]). This would make the sound pressure independent of the excitation frequency with no resonances. Unfortunately, due to the complex geometry, this did not turn out to be the case; the chamber had resonant frequencies. In view of this, it is desirable to fix the excitation frequency and vary the jet velocity to change the excitation Strouhal number. Since the tuning occurs at 40 kHz and 80 m/s the frequency was fixed at 40 kHz. For no other reason than by pure chance this turned out to be a chamber resonance frequency. For comparison purposes, some experiments were conducted at a fixed

Received March 20, 1984; revision received July 2, 1984.

*Research Assistant, St. Anthony Falls Hydraulic Laboratory. Student Member AIAA.
†Research Assistant, St. Anthony Falls Hydraulic Laboratory.
‡Director and Professor, St. Anthony Falls Hydraulic Laboratory. Associate Fellow AIAA.

velocity and changing excitation frequency. When this was done, the excitation voltage was changed so that the output sound pressure was constant.

Polar Correlation

The basic concept involved in this technique is that the axial location of a source can be identified by the cross-spectral density between two far field microphones located on a polar arc centered at the nozzle exit. For a source located downstream of the exit plane, the distance to one of the microphones will be less than it is to the other. The result is a difference in acoustic propagation time and can be related to how far downstream the source is. A fixed microphone is located at $\alpha = 90$ deg and 100 diameters from the nozzle exit. Another microphone is traversed on the same arc away from the fixed microphone and toward the jet axis. The separation angle between the microphones is denoted by β. At each separation angle the cross-spectral density is obtained.

The source location is found by the procedure described by Fisher et al.[4] The details are not included here. For further information see Ref. 5. It is important to note, however, that the basic assumption in the development is that the noise is radiated by small-scale isotropic turbulent eddies that radiate uniformly in all directions. It is found that under the amplified condition in the excited jet, the polar correlation fails to yield a sensible result. This is taken to mean that the sound is produced by a mechanism other than by small-scale turbulent eddies.

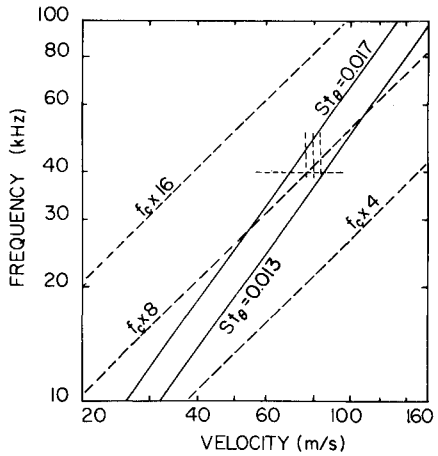

Fig. 1 Coupling between the shear layer instability and the jet column instability.

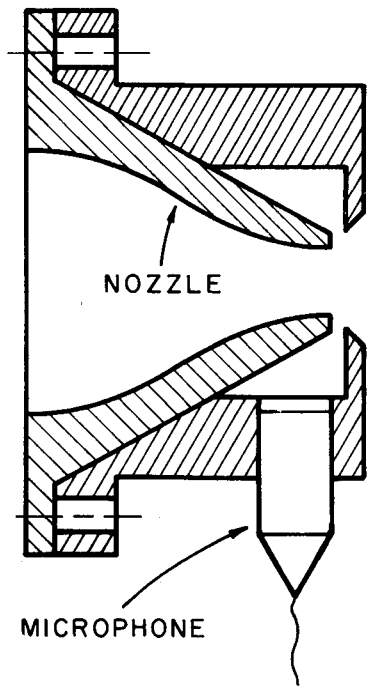

Fig. 2 Exciter chamber assembly.

Results

The change in the level of far field noise with excitation at varying excitation Strouhal numbers is shown in Fig. 3. Qualitatively, the two methods of excitation (changing frequency at constant velocity and changing velocity at constant frequency) produce the same results. Excitation at $St_\theta = 0.013$ increases the noise level by as much as 13 dB with a discrete tone at the first subharmonic. The spectrum is shown in Fig. 4. Comparison with the unexcited spectrum indicates that roughly 6 dB of the total amplification of 13 dB is due to an increase in broadband level. If the flow velocity is increased by ~1 m/s and the jet is excited at the same Strouhal number, other subharmonic spikes appear in the spectrum. This spectrum is shown in Fig. 5. It indicates that excited jets may be extremely sensitive to small changes in conditions. Figure 5 also shows spectra for various emission angles. As the emission

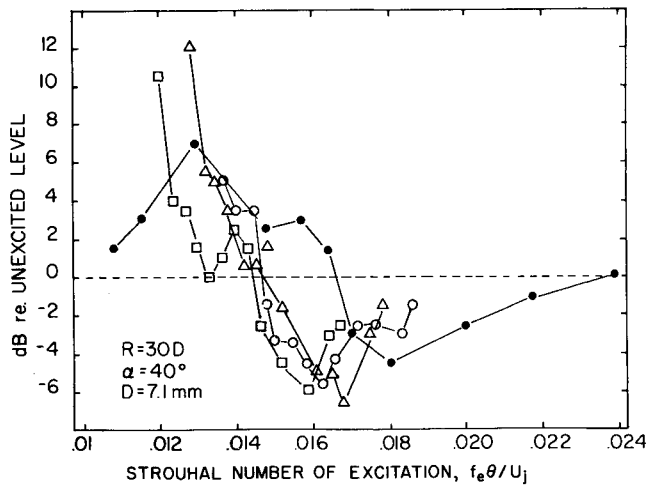

Fig. 3 Change in sound pressure due to excitation. The Strouhal number of excitation $f_e\theta/U_j$ is varied by changing velocity at constant excitation frequency (full circle) or by changing frequency at constant velocity (open symbols). ●: $fe = 40$ kHz; ○: $U_j = 75.5$ m/s; △: $U_j = 79$ m/s; □: $U_j = 83$ m/s.

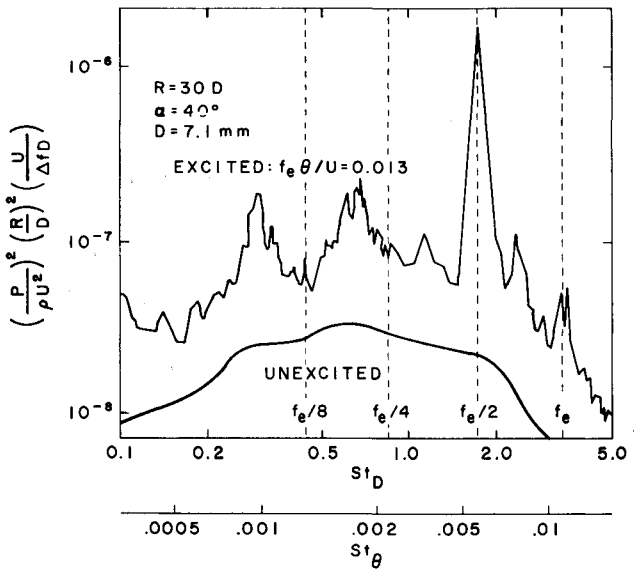

Fig. 4 Far field noise spectrum for the amplification mode.

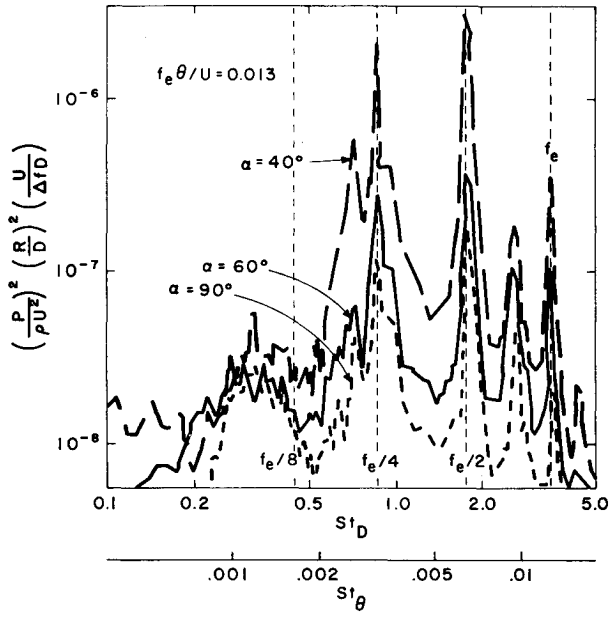

Fig. 5 Far field noise spectrum for the amplification mode including directivity pattern (obtained on a different day than Fig. 4).

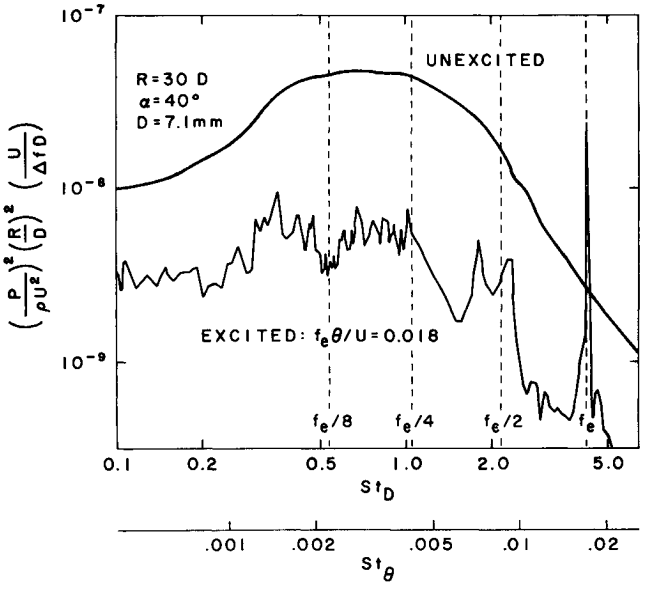

Fig. 6 Far field noise spectrum for the suppressed mode.

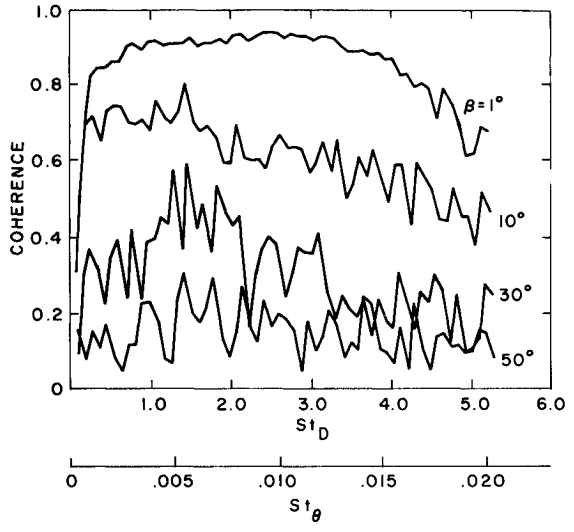

Fig. 7 Coherence of the noise field for the natural jet, β = microphone separation angle.

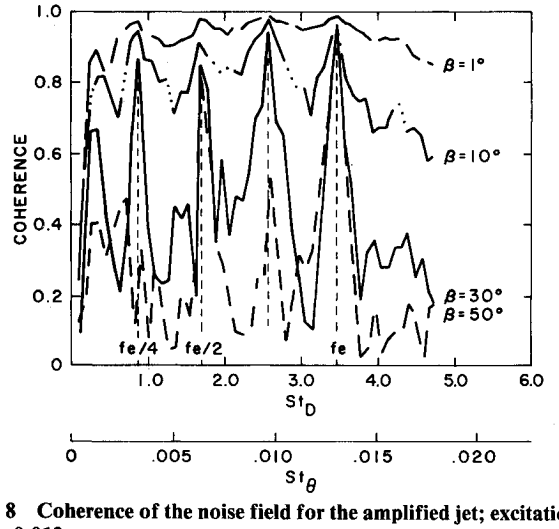

Fig. 8 Coherence of the noise field for the amplified jet; excitation at $St_\theta = 0.013$.

angle changes, it is seen that there is no Doppler shift in the tonal frequencies, implying that the noise originates from stationary sources. Laufer and Yen[6] have inferred that the change in the turbulence associated with these tones is so rapid that it appears that the noise radiates from a fixed point in space.

Excitation at $St_\theta = 0.17$ results in noise suppression by as much as 8 dB with no discrete tones present. The spectrum is shown in Fig. 6. Similar attenuation of the turbulence level in the shear layer has been observed by Zaman and Hussain.[7] This implies that the reduction in turbulence intensity is associated with the reduction in the broadband component of radiated noise. On the other hand, the lack of discrete tones does not imply that the flowfield is void of large-scale structures, but only that the process that produces the tones is lacking. After reviewing the data summary of Crighton,[8] it appears that this is the first time that both broadband amplification and broadband suppression of radiated noise have been observed in the same test rig. This topic is taken up by Long and Arndt.[9]

The coherence of the radiated noise for the three cases, unexcited, amplified, and suppressed, is next explored, as it is the necessary input to the polar correlation. The coherence function is defined by

$$C(f,\beta) = \frac{|CS(f,\beta)|}{[P(f,o)P(f,\beta)]^{1/2}}$$

where $CS(f,\beta)$ is the cross-spectral density, $P(f,\beta)$ the power-spectral density, and β the separation angle between the traversable microphone and a fixed microphone at $\alpha = 90$ deg to the jet axis. Figure 7 shows the coherence for the unexcited jet. The amplitude is relatively independent of frequency and decreases for larger separations. This is not a surprising result, but is necessary for comparison purposes when considering what effect excitation has on the jet structure.

The coherence for the amplified jet is shown in Fig. 8. Strong coherence is observed at the tonal frequencies corresponding to the first and second subharmonics, and at an interaction tone f_a, where $f_a = (f_e/2) + (f_e/4)$. The angular variation of each of these tones is shown in Fig. 9. Evidently, the first subharmonic $f_e/2$ is a different type of source than the second subharmonic $f_e/4$. The highly directional signal implies that the polar correlation technique cannot be used on the amplified jet.

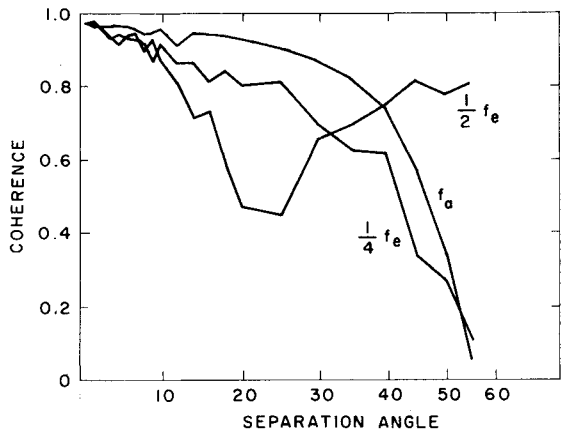

Fig. 9 Angular variation of the coherence at the discrete tones in the amplified jet; excitation at $St_\theta = 0.013$.

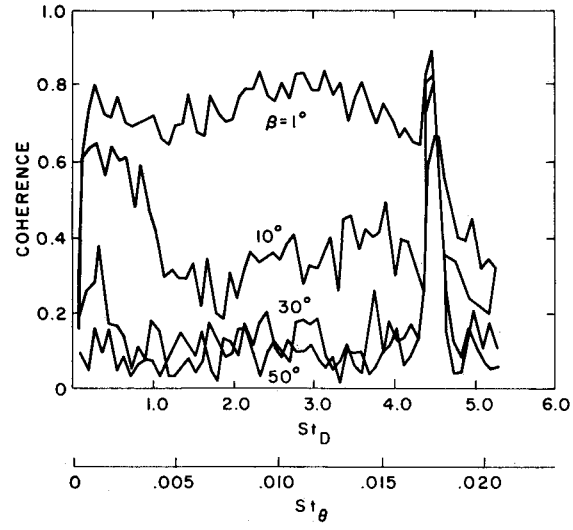

Fig. 10 Coherence of the noise field for the suppressed jet; excitation at $St_\theta = 0.017$.

The coherence of the noise field for the suppressed jet is shown in Fig. 10. Weaker coherence is observed at all frequencies than for the unexcited jet. Even at separations as small as 10 deg, the coherence above $St_D = 1.0$ is less than 0.4. It is only near $St_D = 0.3$ that the coherence is near that for the unexcited jet. This indicates that the jet structure is broken down into more random components than in the natural jet. Zaman and Hussain[7] term this as the "maximum growth rate" mode because it saturates earlier in x and subsequently breaks down into fine grained turbulence. Associated with the decreased coherence is a larger phase shift between the signals received at the two far field microphones. This indic .es that the sound sources have moved further downstream.

The polar correlation provides the axial source location for the unexcited and suppressed jets. This is shown in Fig. 11. As expected, high frequencies are produced near the jet exit and low-frequency noise is radiated further downstream. Excitation at $St_\theta = 0.017$ (suppressed jet) moves the sources at most frequencies downstream by roughly 2 diameters. It is unfortunate that the technique is not able to adequately resolve the location for frequencies less than $St \sim 0.3$, since this is where the bulk of the noise is produced. This is due to the fact that at increasing wavelength the phase difference between the two microphones decreases.

Flow visualization was also used to determine variations in flow structure with excitation. This was accomplished using two smoke wires. One is positioned within the stilling chamber

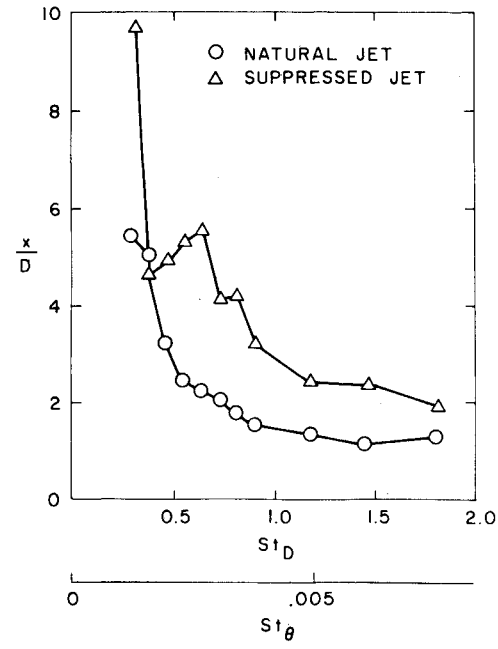

Fig. 11 Axial location of the maximum intensity of the sound sources determined by polar correlation.

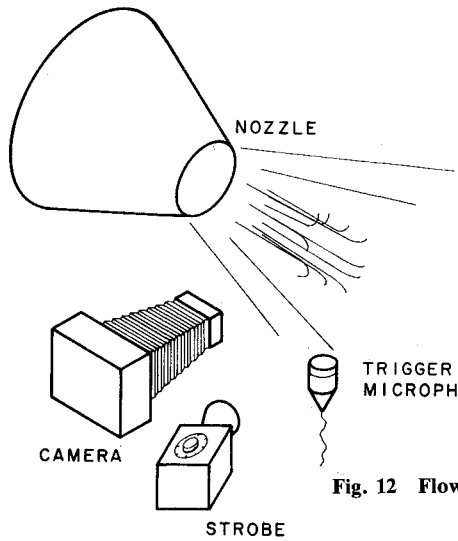

Fig. 12 Flow visualization setup.

of the jet nozzle and feeds smoke into the core region of the jet. A second wire is positioned just downstream of the jet nozzle and permits smoke to be entrained into the shear-layer region. Both wires lay in the plane of photographic observation. The 0.075-mm stainless steel wires are coated with liquid smoke, a substance which is used in model trains for effect. This oil forms distinct beads on the wire and the smoke (oil vapor) burns off from the space between the beads when power is supplied. The interior wire is kinked to fix the location of the beads. Approximately 20 V is supplied for a duration of 0.1 s. This produced a smoke line dense enough to be visible after it had been stretched out by the contraction. The exterior wire was stretched taut between two jewelers broaches. Approximately 12 V of power is supplied for a duration of 0.1 s.

The flow visualization system is shown in Fig. 12. The camera is operated with an open shutter, and the system is triggered by the signal sensed by a microphone located in the hydrodynamic near field of the jet. The sequence of events that produced the photographs of Fig. 13 occurred as follows: with the jet in operation, power is supplied to the wires and the

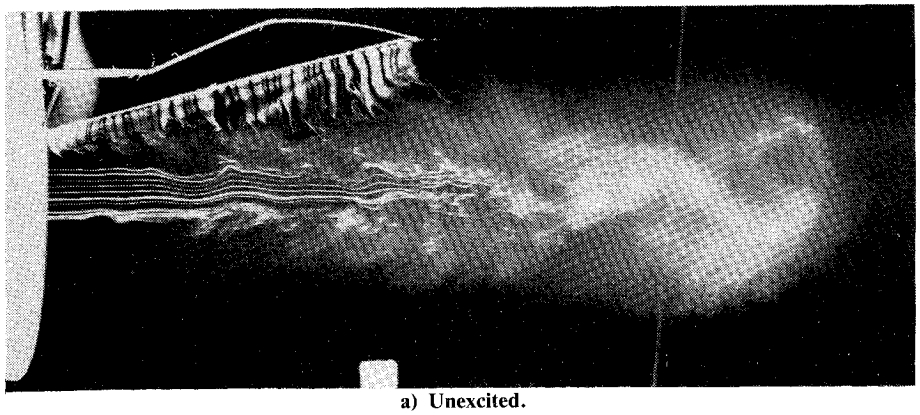

a) Unexcited.

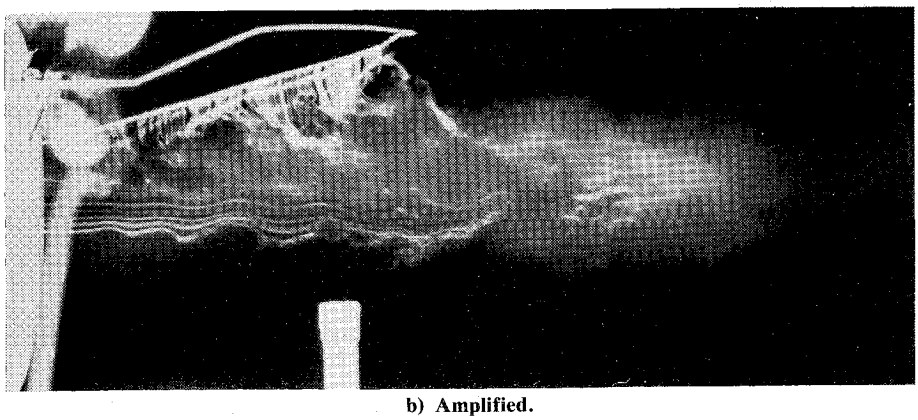

b) Amplified.

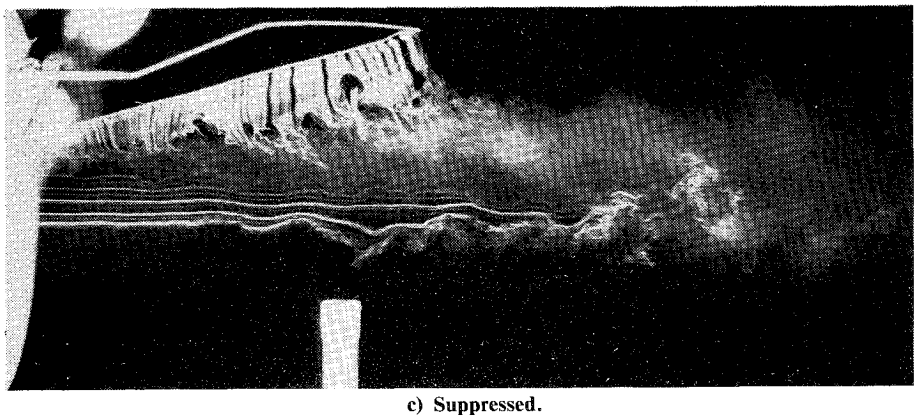

c) Suppressed.

Fig. 13 Flow visualization using smoke wires.

smoke begins to burn off. After a delay of 0.012-ms, which allows the smoke to enter the observation region, the triggering circuitry is switched on. Once the triggering criterion is met, an A/D converter is initiated to record the signal trace. After another preset delay of up to 1000 μ/s, the strobe is flashed and the streaklines are recorded on film. This method allows one to superimpose the time trace of the near-field pressure signal on the photograph to see if a reproducible spatial structure can be linked to the characteristic signal form. It can capture the entire time trace, not just that which occurs after the triggering peak.

The purpose of the conditional sampling was to relate a pressure pulse (or dip) to a single large structure. Results showed that the time trace could not be matched on the photograph. The photographs appeared to be sampled at random rather than being triggered. A similar result has also been observed by Sarohia and Massier.[10] They found that the convection of a single large structure is a weak source of near-field pressure but the interaction of large structures contributes significantly to the near-field pressure.

The results of the flow visualization are in qualitative agreement with the level of broadband noise. This is shown on Fig. 13. The flow development without excitation is shown in Fig. 13a. The most important feature worth noting is the approximate angle at which the smoke lines from the entrainment wire are diffused into the turbulent shear region. This occurs at roughly $\alpha = 10$ deg off the jet axis. The flow development in the amplification mode is shown in Fig. 13b. In this case, the angle at which smoke lines from the entrainment wire enter the turbulent region is much more erratic, but indicates that the spreading angle of the shear region has increased. This implies a more rapid mixing and a higher turbulence level which is consistent with an increased noise level. The suppressed condition is shown in Fig. 13c. The angle of the turbulent region is now less than the unexcited case (Fig. 13a). The jet spreads less rapidly and mixes at a slower rate. This is consistent with the reduced noise level and is in qualitative agreement with the observation that the sound sources have moved downstream.

Conclusion

The jet used in this study is too small for detailed study of the turbulence associated with this amplification/suppression phenomena. Our interest here is in a thorough documentation of the conditions under which the various modes occur along with some qualitative observations concerning the changes in the flow structure.

It has been found that this jet is sensitive to excitation at the shear-layer instability frequencies only when the jet is near the tuned condition shown in Fig. 1. Outside this range there is no effect of excitation; inside this range a variety of phenomena can occur. If the excitation frequency is near $St_\theta = 0.013$, the shear layer spreads rapidly and the noise increases. The spectrum shows discrete tones at various subharmonics of the excitation frequency. These are thought to correspond to consecutive vortex pairing events of ring-like vortices.

If the excitation frequency is near $St_\theta = 0.017$, suppression of the broadband noise results, the shear layer spreads less rapidly, and the sound sources have moved downstream. The slow spreading rate of the shear layer indicates a lack of large-structure interaction in the noise producing region and is consistent with the lack of discrete tones in the spectrum. The fact that the associated broadband noise is decreased indicates that large structures, as well as small structures, are necessary for the production of broadband noise. Moore[11] and Arndt and George[12] came to the same conclusion regarding this large-scale/small-scale interaction. It is also pursued in Ref. 9.

This experiment is a small part of the whole picture concerning jet excitation experiments. In most experiments the tuning criteria used here is not necessary. In some, only suppression is observed[1,6,7]; in others, only amplification is observed.[11] Crighton[8] claimed that the distinction could be made on the basis of the Reynolds number being greater than or less than $\sim 10^5$. The present experiment is in contradiction to this since both phenomena have been observed at a single Reynolds number.

Obviously, other factors must be considered. In particular the Mach number and the initial (exit) conditions are probably important. In view of this it becomes imperative that future excitation experiments be documented thoroughly so that these diverse results can be tied together.

Acknowledgments

This work was supported by the Air Force Office of Scientific Research under Contract F49620-80-C-0053, and the Office of Naval Research under Contract N00014-83-K-0145.

References

[1]Kibens, V., "Discrete Noise Spectrum Generated by an Acoustically Excited Jet," *AIAA Journal*, Vol. 18, April 1980, p. 343.

[2]Long, D. F. and Arndt, R.E.A., "Jet Noise at Low Reynolds Number," *AIAA Journal*, Vol. 22, Feb. 1984, pp. 187-193.

[3]Frederiksen, E., "Condenser Microphones used as Sound Sources," B & K Technical Review, Vol. 3, 1977.

[4]Fisher, M. J., Harper-Bourne, M., and Glegg, S., "Jet Engine Noise Source Location: The Polar Correlation Technique," *Journal of Sound and Vibration*, Vol. 51, 1977, pp. 23-54.

[5]Kim, H., "Sound Source Distributions in Excited and Unexcited Turbulent Jets," M.S. Thesis, University of Minnesota, Minneapolis, Minn., June 1983.

[6]Laufer, J. and Yen, T., "Noise Generation by a Low Mach Number Jet," *Journal of Fluid Mechanics*, Vol. 134, Sept. 1983, pp. 1-34.

[7]Zaman, K.B.M.Q. and Hussain, A.K.M.F, "Turbulence Suppression in Free Shear Flows by Controlled Excitation," *Journal of Fluid Mechanics*, Vol. 103, Feb. 1981, p. 133.

[8]Crighton, D. G., "Acoustics as a Branch of Fluid Mechanics," *Journal of Fluid Mechanics*, Vol. 106, May 1981, p. 261.

[9]Long, D. F. and Arndt, R.E.A., "The Role of Helmholtz Number in Jet Noise," AIAA Paper 84-0403, 1984.

[10]Sarohia, V. and Massier, P. R., "Experimental Results of Large Scale Structures in Jet Flows and Their Relation to Jet Noise Production," *AIAA Journal*, Vol. 16, 1978, p. 831.

[11]Moore, C. J., "The Role of Shear-Layer Instability Waves in Jet Exhaust Noise," *Journal of Fluid Mechanics*, Vol. 80, April 1977, p. 321.

[12]Arndt, R.E.A. and George, W. K., "Investigation of the Large Scale Coherent Structure in a Jet and Its Relevance to Jet Noise," *Proceedings of the 2nd Symposium on Transportation Noise*, Raleigh, N.C., June 1974, p. 142.